AGT

Algebraic & Geometric Topology

Volume 26 (2026)

Linear upper bounds on ribbonlength of knots and links

HYOUNGJUN KIM, SUNGJONG NO AND HYUNGKEE YOO

msp

msp

Algebraic & Geometric Topology **26**:2 (2026) 553–563
DOI: 10.2140/agt.2026.26.553
Published: February 11, 2026

Linear upper bounds on ribbonlength of knots and links

HYOUNGJUN KIM, SUNGJONG NO AND HYUNGKEE YOO

A knotted ribbon is one physical aspect of a knot. A folded ribbon knot is a depiction of a knot obtained by folding a long and thin rectangular strip to become flat. The ribbonlength of a knot type can be defined as the minimum length required to tie the given knot type as a folded ribbon knot. The ribbonlength has been conjectured to grow linearly or sublinearly with respect to a minimal crossing number. Several knot types provide evidence that this conjecture is true, but there is no proof for general cases. In this paper, we show that for any knot or link, the ribbonlength is bounded by a linear function of the crossing number. In more detail,

$$\mathrm{Rib}(K) \leq \tfrac{5}{2}c(K) + 1$$

for a knot or link K. Our approach involves binary grid diagrams and bisected vertex leveling techniques.

1 Introduction

Knot theory, a branch of topology, studies knots and their properties. A *knot* is a simple closed curve in three-dimensional space, and a *link* is a disjoint union of knots. Understanding the properties of knots is useful in many areas of natural science such as physics, biology, chemistry and materials science. One physical aspect of knot theory is the concept of a ribbon structure of a knot. A knotted ribbon represents a geometric measure of its complexity, providing valuable insights into its topological structure [1; 12]. A ribbon structure realizes a ribosomal walking robot [13; 16]. Many circular DNA [8; 9; 10; 14] have knotted ribbon shapes.

Kauffman [5] introduced a *folded ribbon knot*, which represents a knot by folding a long and thin rectangular strip to become flat. By the construction of a folded ribbon knot, the core of the ribbon is piecewise linear as drawn in Figure 1. The ribbonlength can be defined as the minimum length of a long and thin strip of paper required to tie the given knot type. This definition gives us the intuitive notion of tightness of knots, providing a quantitative measure to classify types of knots. Kauffman [5] proposed ribbonlength as drawn in Figure 1. The following definitions were introduced in [3; 4].

Definition Let K be a knot. Then K_w is a *folded ribbon knot* of K with width w that satisfies following two conditions:

(1) The ribbon is flat and its fold lines are disjoint.

(2) The core of K_w is a union of a finite number of consecutively straight lines with crossing information which represents the knot type of K.

MSC2020: 57K10.

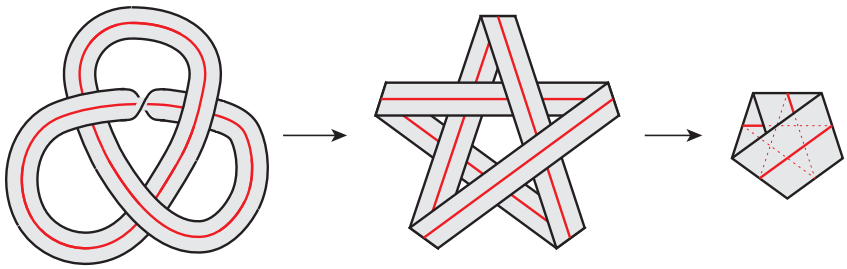

Figure 1: A folded ribbon knot of the trefoil knot.

To define the ribbonlength of a knot or link, the infimum is used rather than the minimum. To see why, consider the trivial knot, which can be represented by folding a ribbon along two parallel lines perpendicular to the core. Then the length of the ribbon can be decreased to an arbitrarily small number.

Definition Take a knot (or link) K and a positive real number w. Then

$$\mathrm{Rib}(K) = \inf_{K' \in [K]_w} \frac{\mathrm{Len}(K'_w)}{w}$$

is called the *ribbonlength* of K where $[K]_w$ is the set of knots (or links) that are equivalent to K and have a folded ribbon knot K'_w.

The upper bound of the ribbonlength of knots has been actively researched. Tian [15] showed that the upper bound of knots is

$$\mathrm{Rib}(K) \leq 2c(K)^2 + 6c(K) + 4,$$

and Denne [2] improved the result. She showed that for any knot or link K,

$$\mathrm{Rib}(K) \leq 72c(K)^{3/2} + 32c(K) + 12c(K)^{1/2} + 4.$$

Furthermore if K is minimally Hamiltonian, then

$$\mathrm{Rib}(K) \leq 9c(K)^{3/2} + 8c(K) + 6c(K)^{1/2} + 4.$$

There are many result for the upper bound of ribbonlength of various families of knots [3; 6; 7]

In this paper, we give an improved upper bound on the ribbonlength of knots which is linear in crossing number.

Theorem 1 *For any knot or link K,*

$$\mathrm{Rib}(K) \leq \tfrac{5}{2}c(K) + 1.$$

Denne [2] mentioned the *ribbonlength crossing number problem* which asks us to find constants c_1, c_2, α, β such that

$$c_1 \cdot c(K)^{\alpha} \leq \mathrm{Rib}(K_w) \leq c_2 \cdot c(K)^{\beta}.$$

She also mentioned that Diao and Kusner conjectured that $\alpha = \frac{1}{2}$ and $\beta = 1$. The authors in [7] have found the partial answer of the conjecture that $\beta = 1$ for a 2-bridge knot or link. The authors in [3] also found a partial answer of the conjecture for the $(2, q)$-torus link and twist knot families. Theorem 1 answers a long held conjecture about the relationship between ribbonlength and crossing number for an arbitrary knot or link.

In Section 2, we introduce binary grid diagrams of knots and links, and a bisected vertex leveling of a plane graph. In Section 3, we explain how to construct the folded ribbon knot, and give lemmas to prove the main theorem. Finally, in Section 4, we find an upper bound of the ribbonlength of knots and links.

2 Preliminary

In this section we define a binary grid diagram. Furthermore, we explain the basic concept of bisected vertex leveling and introduce its relationship with a binary grid diagram.

2.1 Binary grid diagrams

A *grid diagram* is a knot diagram consisting of a finite number of vertical line segments and the same number of horizontal line segments such that each vertical line segment is placed over the horizontal line segments. We introduce a special type of a grid diagram in the following definition.

Definition A *binary grid diagram* is a grid diagram so that each horizontal line segment crosses at most one vertical line segment.

For convenience in recognizing the figures during the proof process, we assume that the horizontal line segment of the binary grid diagram passes over the vertical line segment.

A binary grid diagram can be divided into blocks by cutting horizontally between every pair of consecutive horizontal line segments. That is, each block contains exactly one horizontal line segment and parts of several vertical line segments. Thus each block is represented by six types as drawn in Figure 2, according to the shape of the vertical line segments which meet the horizontal line segment. Such blocks are denoted by B_1, B_2, B_3, $\mathring{B}_1$, $\mathring{B}_2$ and $\mathring{B}_3$.

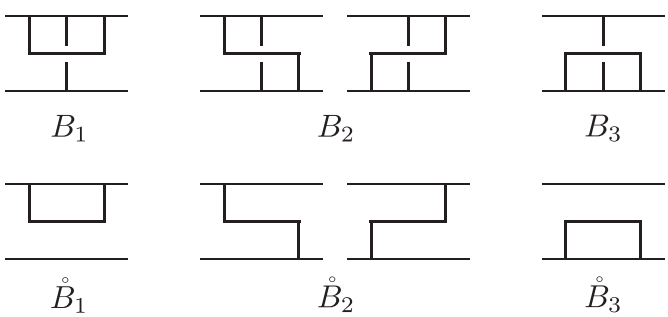

Figure 2: Six types of blocks in a binary grid diagram.

2.2 Bisected vertex leveling

Let G be a connected plane graph which does not have loops. A *bisected vertex leveling* is its ambient isotopy which satisfies the following three conditions:

(1) Each vertex of G lies between two consecutive horizontal lines.

(2) Each edge of G has no maxima and minima as critical points of the height function given by the vertical direction, except its endpoints (vertices).

(3) Each horizontal line cuts G into two pieces, each of which is connected.

The authors [11] first introduced a bisected vertex leveling, and showed the following proposition.

Proposition 2 [11, Theorem 1] *Let G be a connected plane graph without loops. If it has no cut vertex, then G has a bisected vertex leveling.*

A knot projection can be interpreted as a 4-valent plane graph. Let G be such a 4-valent plane graph. If the given knot projection does not have any nugatory crossing, then G has no loop and no cut vertex. Therefore, G has a bisected vertex leveling by the following corollary.

Corollary 3 *For any knot diagram with no nugatory crossing, there is a planar isotopy that transforms the knot diagram to a bisected vertex leveling.*

Any minimal crossing diagram of knots has no nugatory crossing. Therefore, any plane graph corresponding to a knot diagram with minimal crossing has a bisected vertex leveling by Corollary 3.

For the convenience of proofs, we label the portion between consecutive horizontal lines for the diagram of recovering crossing information from G as $T_0^+, \dots, T_4^+, T_0^-, \dots, T_4^-$ as drawn in Figure 3. Moreover, the portion T_i^+ and T_i^- are collectively denoted as T_i^*. By the conditions of a bisected vertex leveling, there is exactly one T_4^* and exactly one T_0^*. This implies that the number of T_3^* is equal to the number of T_1^*.

Remark Each portion T_i^* can be represented by a combination of blocks:

$$
\begin{aligned}
&T_0^* \mapsto \text{a combination of blocks of types } B_1 \text{ and } \mathring{B}_1,\\
&T_1^+ \mapsto \text{a block of type } B_1,\\
&T_1^- \mapsto \text{a combination of blocks of types } \mathring{B}_1 \text{ and } B_2,\\
&T_2^* \mapsto \text{a block of type } B_2,\\
&T_3^+ \mapsto \text{a block of type } B_3,\\
&T_3^- \mapsto \text{a combination of blocks of types } B_2 \text{ and } \mathring{B}_3,\\
&T_4^* \mapsto \text{a combination of blocks of types } B_3 \text{ and } \mathring{B}_3.
\end{aligned}
\tag{1}
$$

Therefore any minimal crossing diagram of knots can be represented as a binary grid diagram.

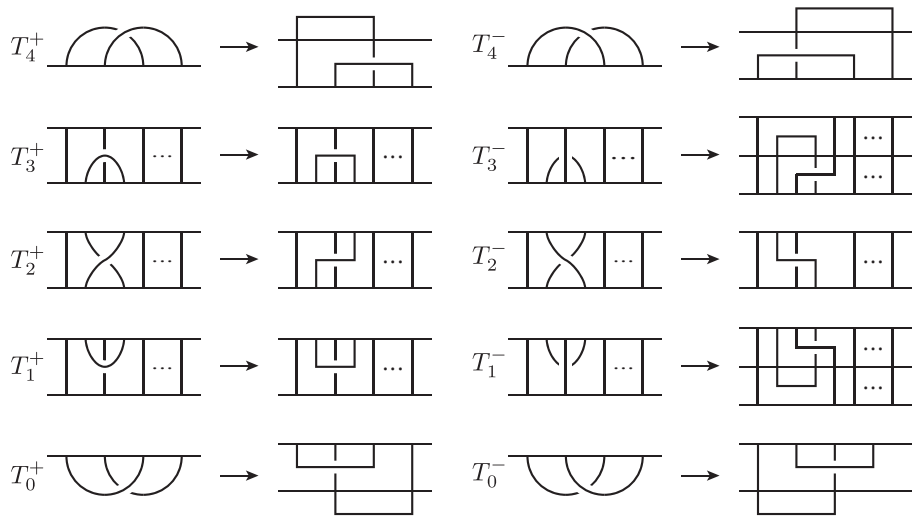

Figure 3: Portions T_i^*'s and their corresponded blocks.

3 Construction

In this section, we explain the construction of a folded ribbon knot from a binary grid diagram. We consider the process of transforming blocks to suitable portions of folded ribbon, and connecting them in the correct order to form the complete folded ribbon knot. The ribbonlength is determined by specific blocks within a binary grid diagram. We introduce some lemmas to derive the main theorem.

Lemma 4 *Let D be a binary grid diagram for knot type of K. If there is a pair of consecutive blocks in which the upper block is of type B_1 or $\mathring{B}_1$, and the lower block is of type $\mathring{B}_3$, then we can switch types of the upper and lower blocks while preserving the knot type of K.*

Proof Suppose that there is a pair of consecutive blocks in which the upper block is of type B_1 or $\mathring{B}_1$, and the lower block is of type $\mathring{B}_3$. Let the horizontal line segments in the upper block and the lower block be $[u_1,u_2]\times\{n+1\}$ and $[l_1,l_2]\times\{n\}$, respectively. If $[l_1,l_2]\cap[u_1,u_2]$ is empty, then switch y-coordinates of the upper and the lower horizontal line segments by using the planar isotopy. Thus, types of the upper and the lower blocks are switched after the above process.

Now we consider the case that $[l_1,l_2]\cap[u_1,u_2]$ is not empty. First assume that the upper block is of type B_1. Let c be an x-coordinate of the vertical line segment which is passing through the horizontal line segment in B_1. Since the lower horizontal line segment does not cross this vertical line segment, there are two cases: $l_2\in[u_1,c]$ and $l_1\in[c,u_2]$.

For the first case $l_2\in[u_1,c]$, we take the piecewise linear line P as drawn in Figure 4(a). In detail, P consists of two rays $\{u_1-\frac{1}{2}\}\times[n+1,\infty)$ and $\{l_2+\frac{1}{2}\}\times(-\infty,n]$, and the line segment between them. We partition the plane into three distinct regions, namely R, R_-, and R_+, based on the ε-tubular neighborhood R of P. Here, R_- and R_+ correspond to the left and right regions of the complement of R, respectively. Through a planar isotopy, we expand R and translate R_+ horizontally until the boundary

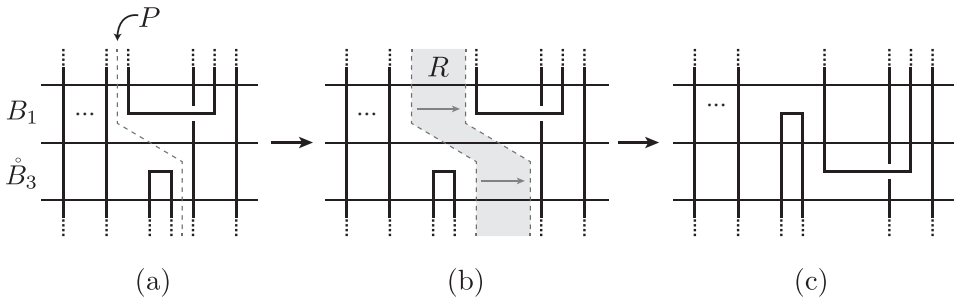

Figure 4: A switching process of the upper and lower blocks.

between R and R_+ is translated by $l_2 - u_1 + 1$ in the x direction while keeping R_- fixed as drawn in Figure 4(b). Now we adjust the horizontal spacing of the diagram so that the vertical line segments are spaced by units apart. Then we can switch types of the upper and lower blocks similar with the case of $[l_1, l_2] \cap [u_1, u_2] = \varnothing$ as drawn in Figure 4(c). For the second case $l_1 \in [c, u_2]$, we take the piecewise linear line P which consists of two rays $\{u_2 + \frac{1}{2}\} \times [n+1, \infty)$ and $\{l_1 - \frac{1}{2}\} \times (-\infty, n]$, and the line segment between them. We can also switch the types of the upper and lower blocks similar with the first case.

It remains to consider the case that the upper block is of type $\mathring{B}_1$. To address this case, we use the same argument in any case where the upper block is of type B_1. Then we can switch the types of the upper and lower blocks while preserving the knot type of K. □

We can transform blocks of types B_2 and B_3 to combinations of blocks of types B_1 and $\mathring{B}_3$ as drawn in Figure 5. So we obtain the following lemma.

Lemma 5 *Let D be a binary grid diagram for knot type of K. Then there exists an algorithm that converts D into another binary grid diagram consisting of blocks of types B_1, $\mathring{B}_1$, and $\mathring{B}_3$ while maintaining the total number of all blocks of types B_1, B_2, B_3 and $\mathring{B}_1$.*

Now we introduce a particular object to construct the folded ribbon knot. A *paper plane* is a folded ribbon obtained by folding a piece of ribbon three times as shown in Figure 6. In the figure on the left, the darker regions on the two ends of the paper plane can be made as long or as short as needed in order to join

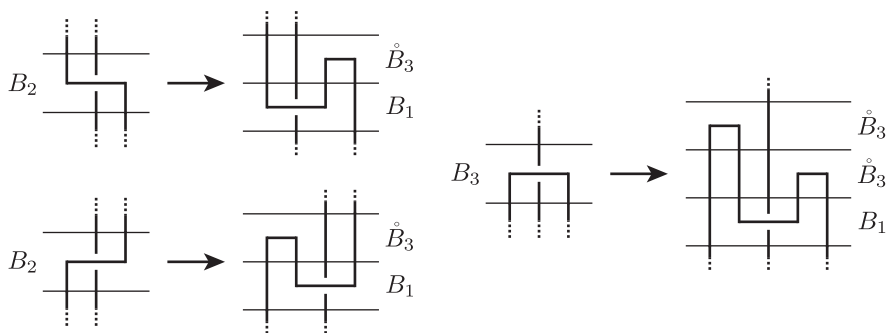

Figure 5: Transforming blocks of types B_2 and B_3.

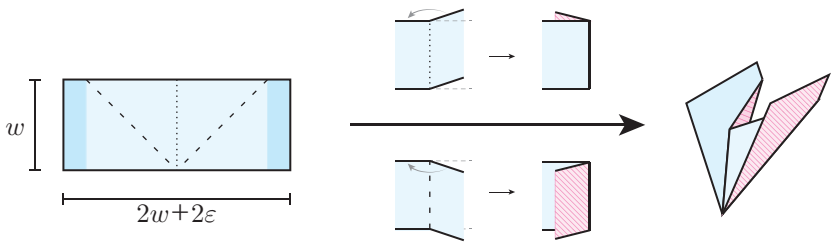

Figure 6: A structure of a paper plane.

different paper planes together. These regions are called *wings*. The horizontal line segment of a block of type B_1 or $\mathring{B}_1$ can be represented by a paper plane, while the vertical line segments correspond to wings.

Lemma 6 *Let D be a binary grid diagram for knot type of K. Then*

$$\mathrm{Rib}(K) \le 2(b_1 + b_2 + b_3 + \mathring{b}_1),$$

where b_i and $\mathring{b}_1$ are the number of blocks of type B_i and $\mathring{B}_1$ in D, respectively.

Proof Let D be a binary grid diagram of a knot K as drawn in Figure 7(a). By Lemma 5, we convert all blocks of types B_2 and B_3 to combinations of blocks of types B_1 and $\mathring{B}_3$ as drawn in Figure 7(b). Then we rearrange blocks such that all blocks of type $\mathring{B}_3$ are lying above the other types by Lemma 4 as drawn in Figure 7(c). We write D' for the resulting diagram. Let the upper part of D' be the part consisting of all blocks of type $\mathring{B}_3$, and the lower part of D' be the other.

Now we represent a folded ribbon knot with width w from D'. We divide the remaining proof into three parts.

Step I: *transforming the lower part of D' into paper planes*. The i-th *stack* is a part of the rearranged D' which consists of i blocks from the bottommost block. We denote the i-th stack as S_i. To construct a

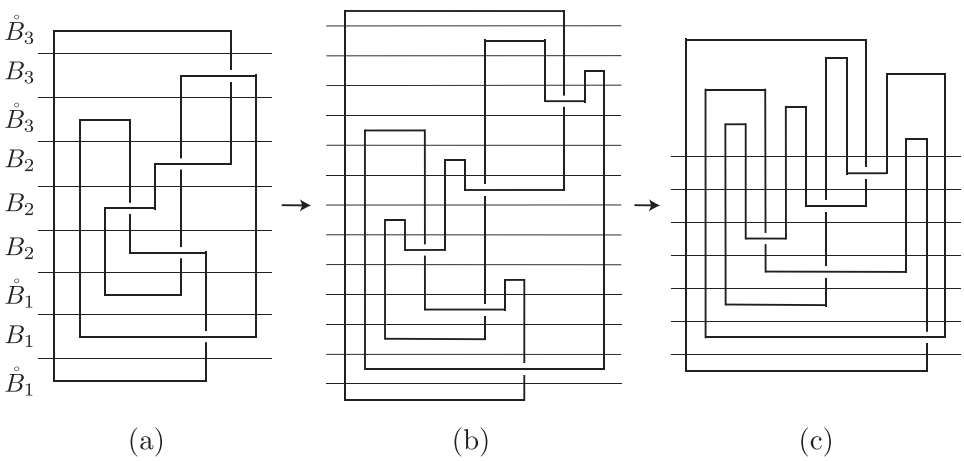

Figure 7: The converted binary grid diagram D'.

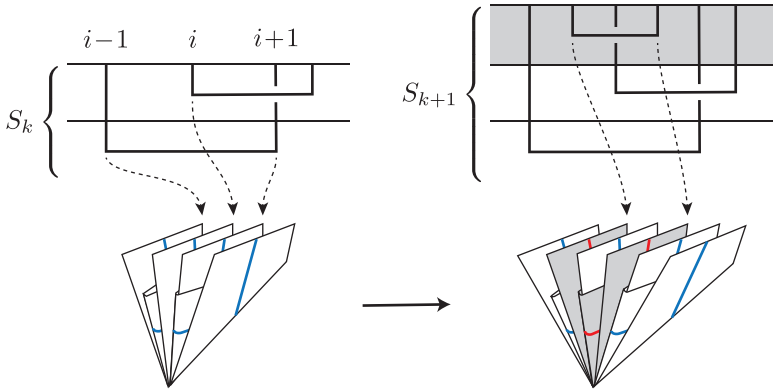

Figure 8: Constructing S_{k+1} from S_k by inserting a paper plane.

ribbon knot, we first transform all blocks in the lower part of D' into paper planes. We use a sequential process superimposing a new paper plane to the former stack. So we need the empty space for inserting the new paper plane, call this space an *insertable space*.

We aim to demonstrate, through induction, that the k-th stack S_k can be represented by a particular arrangement of k paper planes. In this arrangement, all wings are oriented upward, and there are insertable spaces between every pair of consecutive wings for the next paper plane. Such an arrangement is called a *pile of k paper planes*. The bottommost layer is always composed of $\mathring{B}_1$, and there exists an insertable space between the wings of $\mathring{B}_1$, establishing the initial step.

Now assume that S_k has been represented by a pile of k paper planes and there is an insertable space between every pair of consecutive wings for the next paper plane. Then we proceed to implement the appearance up to the $(k+1)$-th block by adding one more paper plane.

Suppose that the $(k+1)$-th block is of type B_1. Then its horizontal line segment only crosses a single vertical line segment. There is a wing in the pile of k paper planes, say the i-th wing in order from left to right, which is corresponding to the such vertical line segment. We insert each wing of the new paper plane into the insertable space. In detail, the left wing is inserted between the $(i-1)$-th wing and the i-th wing, and the right wing is inserted between the i-th wing and the $(i+1)$-th wing as drawn in Figure 8. Here if the i-th wing is the leftmost (resp. rightmost) wing, then the left (resp. right) wing of the new paper plane is inserted in the left (resp. right) space of the pile of k paper planes. Thus we have constructed the pile of $k+1$ paper planes which represents S_{k+1}. We note that this new pile has $2k+2$ wings, and there is an insertable space between each consecutive wing.

It remains to consider that the $(k+1)$-th block is of type $\mathring{B}_1$. Then there are two cases according to the location of the horizontal line segment of $(k+1)$-th block. The first case is that the horizontal line segment is lying between two consecutive vertical line segments of S_k. Then there are two wings in the pile of k paper planes, say the i-th and the $(i+1)$-th wing, which correspond to these vertical line segments. We insert both wings of the new paper plane into the insertable space between the i-th wing and the $(i+1)$-th wing. The second case is that the horizontal line segment is lying in the left (resp. right)

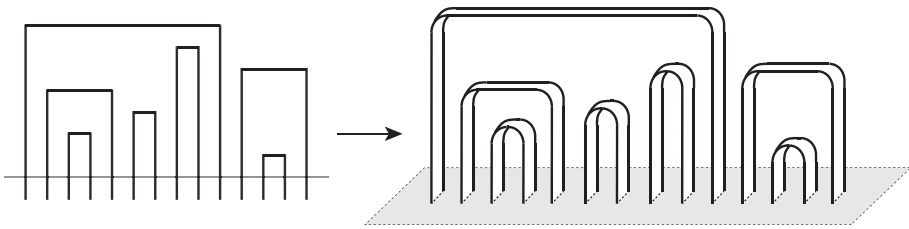

Figure 9: Transforming the upper part of D'.

of the leftmost (resp. rightmost) vertical line segments of S_k. Then we attach the new paper plane to the left (resp. right) of the pile of k paper planes. So we obtain the pile of $k+1$ paper planes which represents S_{k+1}. We note that this new pile has $2k+2$ wings, and there is an insertable space between each consecutive wing.

Step II: *construction of a folded ribbon knot from* D'. We transform the upper part of D' into the product of the set of arcs in this part with an interval of width w as drawn in Figure 9. Then it is represented as a union of ribbons with the same number of paper planes. We connect the upper part and the lower part from left to right sequentially to construct a folded ribbon knot. This process guarantees that the core of the resulting folded ribbon knot is same with the diagram D'.

Step III: $\mathrm{Rib}(K) \leq 2(b_1 + b_2 + b_3 + \mathring{b}_1)$ *where* b_i *and* $\mathring{b}_1$ *are the number of blocks of type* B_i *and* $\mathring{B}_1$ *in* D, *respectively*. Note that both binary grid diagrams D and D' have the same knot type of K. So we check the ribbonlength of a folded ribbon knot which is constructed in Step II. This folded ribbon knot consists of paper planes representing blocks of types B_1 and $\mathring{B}_1$, and their connections. Since the length of each wing and each connection can be made sufficiently small, the length of the folded ribbon can be reduced to the total length of paper planes. Note that the length of each paper plane is equal to 2. Since the folded ribbon knot is constructed by D', it contains the same number of paper planes as the total number of blocks of type B_1 and $\mathring{B}_1$ in D'. This also equals the total number of blocks of type B_1, B_2, B_3 and $\mathring{B}_1$ in D by Lemma 5. Thus a folded ribbon knot of K is represented by $\mathrm{Rib}(K) \leq 2(b_1 + b_2 + b_3 + \mathring{b}_1)$. □

4 An upper bound of ribbonlength

In this section, we find an upper bound on the ribbonlength of knots and links in terms of the crossing number of knots and links, thus proving Theorem 1. Let K be a knot or link. Then K can be represented as a minimal crossing diagram which includes exactly one T_0^* and exactly one T_4^* by using the bisected vertex leveling. As mentioned in Section 2.2, all portions T_i^* are transformed into combinations of blocks to represent K as a binary grid diagram. We remark that ribbonlength is only affected by the number of blocks of types B_1, B_2, B_3 and $\mathring{B}_1$. Thus a bisected vertex leveling with smaller number of T_1^- is efficient to find the sharper upper bound of ribbonlength, since it has exactly one T_0^*.

Now we introduce the transformations the x-flip and the y-flip for a diagram obtained from the bisected vertex leveling of K as drawn in Figure 10. Here, we consider the diagram is embedded in the

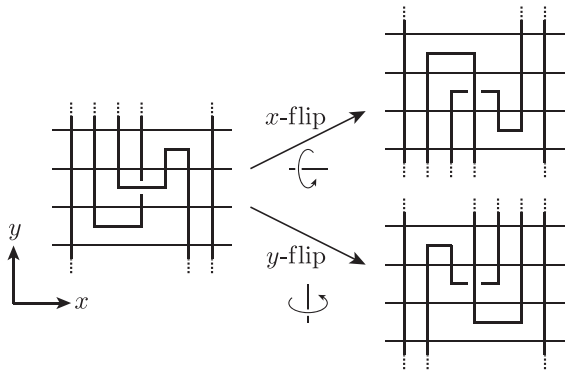

Figure 10: Rotating transformations the x-flip and the y-flip.

three-dimensional space $\mathbb{R}^3$, and also consider the rotations in this space. The x-flip and the y-flip denote transformations of a knot diagram that rotates about the x-axis and the y-axis through π, respectively. The x-flip and the y-flip change the crossing information. The x-flip exchanges T_i^* and T_{4-i}^*, and the y-flip exchanges T_i^* and T_i^* for $i = 1\ldots,4$. Especially the x-flip and the y-flip exchange T_1^* and T_3^* as in the following table:

type of flips	exchanging operation
x-flip	$T_1^+ \leftrightarrow T_3^-,\ T_1^- \leftrightarrow T_3^+$
y-flip	$T_1^+ \leftrightarrow T_1^-,\ T_3^+ \leftrightarrow T_3^-$

This implies that we can change the knot diagram using the x-flip and the y-flip such that the smallest number among T_1^+, T_1^-, T_3^+ and T_3^- becomes T_1^-. Since the knot diagram includes exactly one of each of T_0^* and T_4^*, the x-flip and the y-flip do not change each of those numbers. This implies that the number of T_1^- is at most $\lfloor \frac{1}{4}(c(K)-2) \rfloor$ in the changed knot diagram. By the remark in Section 2.2, each portion of T_0^* and T_1^- is transformed into two blocks among types B_1, B_2, B_3 and $\mathring{B}_1$. Moreover each of the other portions is transformed into one or two blocks which contains exactly one block among these four types. Thus the binary grid diagram obtained from this knot diagram includes at most $c(K)+1+\lfloor \frac{1}{4}(c(K)-2) \rfloor$ blocks among types B_1, B_2, B_3 and $\mathring{B}_1$. By Lemma 6,

$$\begin{aligned} \mathrm{Rib}(K) &\leq 2(b_1+b_2+b_3+\mathring{b}_1) \\ &\leq 2\big(c(K)+1+\lfloor \tfrac{1}{4}(c(K)-2) \rfloor\big) \\ &\leq \tfrac{5}{2}c(K)+1, \end{aligned}$$

where b_i and $\mathring{b}_1$ are the number of blocks of type B_i and $\mathring{B}_1$ in D, respectively.

Acknowledgements

Hyoungjun Kim was supported by the National Research Foundation of Korea (NRF) grant funded by the Korea government Ministry of Science and ICT(RS-2021-NR061671). Sungjong No was supported by the National Research Foundation of Korea (NRF) grant funded by the Korea government Ministry

of Science and ICT (NRF-2020R1G1A1A01101724). The corresponding author Hyungkee Yoo was supported by Basic Science Research Program of the National Research Foundation of Korea (NRF) grant funded by the Korea government Ministry of Education (RS-2023-00244488).

References

[1] **K C Cheung**, **E D Demaine**, **J R Bachrach**, **S Griffith**, *Programmable assembly with universally foldable strings (moteins)*, Trans. Rob. 27:4 (2011) 718–729

[2] **E Denne**, *Ribbonlength and crossing number for folded ribbon knots*, J. Knot Theory Ramifications 30:4 (2021) art. id. 2150028 MR

[3] **E Denne**, **J C Haden**, **T Larsen**, **E Meehan**, *Ribbonlength of families of folded ribbon knots*, Involve 15:4 (2022) 591–628 MR

[4] **E Denne**, **M Kamp**, **R Terry**, **X Zhu**, *Ribbonlength of folded ribbon unknots in the plane*, from "Knots, links, spatial graphs, and algebraic invariants" (E Flapan, A Henrich, A Kaestner, S Nelson, editors), Contemp. Math. 689, Amer. Math. Soc., Providence, RI (2017) 37–51 MR

[5] **L H Kauffman**, *Minimal flat knotted ribbons*, from "Physical and numerical models in knot theory" (J A Calvo, K C Millett, E J Rawdon, A Stasiak, editors), Ser. Knots Everything 36, World Sci., Singapore (2005) 495–506 MR

[6] **H Kim**, **S No**, **H Yoo**, *Ribbonlength of twisted torus knots*, J. Knot Theory Ramifications 31:12 (2022) art. id. 2250092 MR

[7] **H Kim**, **S No**, **H Yoo**, *Folded ribbonlength of 2-bridge knots*, J. Knot Theory Ramifications 32:4 (2023) art. id. 2350030 MR

[8] **N C H Lim**, **S E Jackson**, *Molecular knots in biology and chemistry*, J. Phys.: Condens. Matter 27 (2015) art. id. 354101

[9] **L F Liu**, **C-C Liu**, **B M Alberts**, *Type II DNA topoisomerases: enzymes that can unknot a topologically knotted DNA molecule via a reversible double-strand break*, Cell 19:3 (1980) 697–707

[10] **L F Liu**, **L Perkocha**, **R Calendar**, **J C Wang**, *Knotted dna from bacteriophage capsids*, Proc. Natl. Acad. Sci. USA 78:9 (1981) 5498–5502

[11] **S No**, **S Oh**, **H Yoo**, *Bisected vertex leveling of plane graphs: braid index, arc index and delta diagrams*, J. Knot Theory Ramifications 27:8 (2018) art. id. 1850044 MR

[12] **A Reid**, **F Lechenault**, **S Rica**, **M Adda-Bedia**, *Geometry and design of origami bellows with tunable response*, Phys. Rev. E 95:1 (2017) art. id. 013002

[13] **S Risi**, **D Cellucci**, **H Lipson**, *Ribosomal robots: evolved designs inspired by protein folding*, from "Proceedings of the 15th Annual Conference on Genetic and Evolutionary Computation" (Amsterdam, 2013), Association for Computing Machinery, New York (2013) 263–270

[14] **J E Stray**, **N J Crisona**, **B P Belotserkovskii**, **J E Lindsley**, **N R Cozzarelli**, *The saccharomyces cerevisiae Smc2/4 condensin compacts dna into (+) chiral structures without net supercoiling*, J Biol Chem. 280:41 (2005) 34723–34734

[15] **G Tian**, *Linear upper bound on the ribbonlength of torus knots and twist knots*, preprint (2018) arXiv 1809.02095

[16] **L Wang**, **M M Plecnik**, **R S Fearing**, *Robotic folding of 2D and 3D structures from a ribbon*, from "2016 IEEE International Conference on Robotics and Automation (ICRA)" (Stockholm, 2016), IEEE Press (2016) 3655–3660

HYOUNGJUN KIM kimhjun@knu.ac.kr
Department of Mathematics Education, Kyungpook National University, Daegu, South Korea

SUNGJONG NO sungjongno@kgu.ac.kr
Department of Mathematics, Kyonggi University, Suwon, South Korea

HYUNGKEE YOO hyungkee@scnu.ac.kr
Department of Mathematics Education, Sunchon National University, Suncheon, South Korea

Received: March 19, 2024 Revised: December 16, 2024

ALGEBRAIC & GEOMETRIC TOPOLOGY

msp.org/agt

See inside back cover or msp.org/agt for submission instructions.

The subscription price for 2026 is US $795/year for the electronic version, and $1170/year (+$80, if shipping outside the US) for print and electronic. Subscriptions, requests for back issues and changes of subscriber address should be sent to MSP. Algebraic & Geometric Topology is indexed by Mathematical Reviews, Zentralblatt MATH, Current Mathematical Publications and the Science Citation Index.

Algebraic & Geometric Topology (ISSN 1472-2747 printed, 1472-2739 electronic) is published 9 times per year and continuously online, by Mathematical Sciences Publishers, 2000 Allston Way # 59, Berkeley, CA 94701-4004. Periodical rate postage paid at Oakland, CA 94615-9651, and additional mailing offices. POSTMASTER: send address changes to Mathematical Sciences Publishers, 2000 Allston Way # 59, Berkeley, CA 94701-4004.

AGT peer review and production are managed by EditFlow® from MSP.

PUBLISHED BY

mathematical sciences publishers

nonprofit scientific publishing

https://msp.org/

ALGEBRAIC & GEOMETRIC TOPOLOGY

Volume 26 Issue 2 (pages 411–824) 2026